

MIT Open Access Articles

General characteristics of tropospheric trace constituent layers observed in the MOZAIC program

The MIT Faculty has made this article openly available. **Please share** how this access benefits you. Your story matters.

Citation: Thouret, Valérie et al. "General Characteristics of Tropospheric Trace Constituent Layers Observed in the MOZAIC Program." *Journal of Geophysical Research: Atmospheres* 105, D13 (July 2000): 17379–17392 © 2000 American Geophysical Union (AGU)

As Published: <http://dx.doi.org/10.1029/2000JD900238>

Publisher: American Geophysical Union (AGU)

Persistent URL: <http://hdl.handle.net/1721.1/111075>

Version: Final published version: final published article, as it appeared in a journal, conference proceedings, or other formally published context

Terms of Use: Article is made available in accordance with the publisher's policy and may be subject to US copyright law. Please refer to the publisher's site for terms of use.



General characteristics of tropospheric trace constituent layers observed in the MOZAIC program

Valérie Thouret, John Y. N. Cho, and Reginald E. Newell

Department of Earth, Atmospheric, and Planetary Sciences, Massachusetts Institute of Technology, Cambridge

Alain Marengo

Laboratoire d'Aérodynamique, Université Paul Sabatier, Toulouse, France

Herman G. J. Smit

Research Center Julich, Institute for Chemistry of the Polluted Atmosphere, Julich, Germany

Abstract. We present a statistical study on tropospheric layers as allowed by the most extensive ozone and water vapor database currently available. Considering O_3 and H_2O deviations from an automatically calculated background, we define four types of layers. These tropospheric layers are a common feature, with the percentage of the troposphere occupied by such layers varying from 7% to 33% depending on the region and the season. Most of the layers are found between 4 and 8 km altitude, and the median thickness is about 500 m. At northern midlatitudes we find 4 times more layers in summer than in winter, while in tropical Asia we observe a spring maximum in the occurrence of the layers. The most abundant layer type everywhere is O_3+H_2O- and corresponds to the signature of stratospheric intrusions or continental pollution. This suggests that stratosphere-troposphere exchanges or at least their influence are not negligible in summer at midlatitudes or in the tropics. A complete understanding of the layers could lead to a better empirical assessment of the different tropospheric ozone sources and to an assessment of the potential vorticity fluxes in the troposphere.

1. Introduction

The atmosphere is full of layered structures of various kinds, from sodium layers near the mesopause [Bernard, 1938] to submeter-scale temperature and humidity sheets in the lower troposphere [Muschinski and Wode, 1998]. Our study deals with trace constituent layers in the troposphere. While stratospheric ozone laminae are hypothesized to be generated by differential advection against a background vertical tracer gradient [Danielsen *et al.*, 1991; Newman and Schoeberl, 1995], the tropospheric layers are thought to originate from surface sources plus convection and capping, stratospheric sources plus intrusion and fragmentation, and other such combinations of source plus advection mechanism.

Previously, the NASA Global Tropospheric Experiment (GTE) Pacific Exploratory Missions (PEM) data were used to study different layer types [Newell *et al.*,

1996; Wu *et al.*, 1997; Stoller *et al.*, 1999]. Then the use of the more extensive ozone and water vapor data bank provided by the Measurement of Ozone and Water Vapor by Airbus In-Service Aircraft (MOZAIC) program [Marengo *et al.*, 1998] revealed the ubiquity of such layers in the troposphere [Newell *et al.*, 1999]. Layers defined with ozone and water vapor are found everywhere, all the time, and occupy 14–20% of the troposphere from 2 to 12 km altitude [Newell *et al.*, 1999]. Using ozone and water vapor measurements, we can define four types of layers with different combinations of positive or negative deviations from the automatically calculated background vertical profile. An explanation of the current algorithm and some examples are given in section 2 and by Stoller *et al.* [1999].

We will refer to ozone-rich and water-vapor-rich (O_3+H_2O+) layers as type 1; to ozone-rich and water-vapor-poor (O_3+H_2O-) layers as type 2; to ozone-poor and water-vapor-rich (O_3-H_2O+) layers as type 3; and to ozone-poor and water-vapor-poor (O_3-H_2O-) layers as type 4. The type 1 layers should be characteristic of convection from the polluted boundary layer. Type 2 could have two possible origins: the stratosphere and polluted continental air. The most likely origin of type 3

Copyright 2000 by the American Geophysical Union.

Paper number 2000JD900238.
0148-0227/00/2000JD900238\$09.00

is convective motions which carry unpolluted boundary layer air aloft that stabilizes in the free troposphere. Type 4 is probably clean marine air that has undergone subsidence. We already know that type 2 layers are the most abundant everywhere in the 2–12 km altitude range in regions studied with MOZAIC and PEM data [Newell *et al.*, 1999].

We believe these layers to be important players in both dynamical and chemical processes in several respects. First, from a transport perspective, layers may contain significant fractions of pollution and stratospheric air that have not yet been well mixed into the tropospheric background. Current models that cannot resolve such layers would not be able to accurately represent the actual advection that takes place. Layers may also be involved in the transport of dynamical quantities such as momentum and potential vorticity (PV) at the same time. Second, nonlinear photochemical reaction rates for crucial species such as ozone imply that not resolving the layer structures can produce inaccuracies in the net production/destruction of the species. Third, the sharp concentration gradients in radiatively important species at the top and bottom of the layers can generate substantial differential heating/cooling that can alter the stability of the layer and its environment (water vapor is the most important gas in this case). For example, wet layers can generate clear-air turbulence, while dry layers create a self-stabilizing motion and thus influence the general circulation. Furthermore, dry and wet layers can add or subtract nontrivially to the net amount of radiative cooling to space of the order of up to 8 W m^{-2} (J. Cho and R. Newell, unpublished data, 2000).

The availability of the MOZAIC measurements (see details in section 2) allows us to go further in the interpretations. The MOZAIC program data help us to focus, for example, on seasonal and regional variations and to complete the statistical study started previously with the PEM data. The 3.5 years of regular measurements “worldwide” allow a reliable statistical study about the general characteristics (mean altitude, mean thickness, etc.) of these tropospheric layers in order to help us understand the origin of this stratification. In this paper we will give for the first time a global characterization of this relatively new finding we call tropospheric trace constituent layers.

2. Data Set and Layer Detection Algorithm

The MOZAIC program was designed especially to collect ozone and water vapor data, using automatic equipment installed aboard five long-range Airbus A340 aircraft flying regularly all over the world [Marenco *et al.*, 1998]. The program started in August 1994, and the data set used for this study corresponds to measurements of ozone and water vapor recorded between August 1994 and December 1997. For this study we

only used vertical profiles corresponding to takeoff and landing phases in the vicinity of about 50 airports visited by MOZAIC aircraft. Most of the MOZAIC data have been recorded at northern midlatitudes (Europe, North America, China, and Japan), but the program also provides data in the northern tropics (northern South America, Africa, and the Indo Asian subcontinent) and in the Southern Hemisphere, mostly Brazil and South Africa. For further details, see Marenco *et al.* [1998]. A map of the coverage is given by Marenco *et al.* [1998] and Cho *et al.* [1999a] and is available from the MOZAIC Web site (<http://www.aero.obs-mip.fr/mozaic/>).

The accuracy and resolution of ozone and water vapor measurements allow us to define very well the small-scale vertical structures involved in this study. The MOZAIC program provides measurements every 4 s for both ozone and water vapor, and given that the vertical speed of the aircraft is around $5\text{--}7 \text{ m s}^{-1}$, the vertical resolution of the data is about 20–28 m. For ozone a dual-beam UV absorption instrument (Thermo-Electron, model 49-103) is used, and the measurement accuracy was estimated at $\pm 2 \text{ ppbv} + 2\%$; details are given by Thouret *et al.* [1998a]. For water vapor a capacitive relative humidity sensor (Humicap -H, Vaisala) is used, and overall uncertainties are within $\pm 4\text{--}7\%$, as described in detail by Helten *et al.* [1998].

In order to analyze atmospheric layers, in terms of correlations or anticorrelations between ozone and water vapor, we determined automatically for each vertical profile a background profile. Definitions of the different types of layers may be made by considering positive or negative ozone and water vapor deviations from this background. Altitude and thickness of the layers are drawn only from the ozone profiles. The water vapor profiles are only used to check if the deviation in H_2O is positive or negative (i.e., if the ozone layer detected is dry or not). In that way, we are avoiding the problems related to the water vapor sensor time response as discussed by Iselin and Gutowski [1997] when studying only water vapor layers.

The minimum deviations required for defining a layer are 10 ppbv for ozone and 5% relative humidity for water vapor. Even though this last criterion is similar to the uncertainty in humidity measurement, this water vapor deviation is sufficient for identifying a layer. Several deviations have been tested (from 5% to 20%), as shown by Newell *et al.* [1999], and even if the the number of layers decreases when H_2O deviation increases, there is almost no change in the resulting statistics. For both background calculations and layer analyses we neglected the lowest 2 km of the troposphere to avoid defining the boundary layer as a layer in our statistics, so our sampling of layers is not contaminated by the fact that measurements are taken near the major sources of pollution (big cities). We also avoided defining the lower stratosphere as a layer by stopping both the layer-finding algorithm and the counting of vertical distance

Table 1. Regional Differences

	Europe 40°–60°N 5°W–25°E	Eastern United States 35°–60°N 90°–60°W	China- Japan 30°–60°N 100°–180°E	Southern United States 20°–35°N 110°–90°W	Tropical Asia 5°S–25°N 70°–120°E	Tropical America 20°S–20°N 90°–60°W	Tropical Africa 20°S–20°N 0°–60°E	Southern Hemisphere 0°–30°S 60°W–60°E	All
Number of observations									
Type 1	1396	514	266	156	312	174	95	400	3460
Type 2	5595	1881	830	496	849	425	265	980	11853
Type 3	1930	569	265	163	274	129	107	262	3931
Type 4	1603	850	306	295	258	138	79	511	4288
Percentage of observations									
Type 1	13	13	16	14	18	20	17	18	15
Type 2	54	50	50	45	50	49	49	46	50
Type 3	18	15	16	15	16	15	20	12	17
Type 4	15	22	18	26	16	16	14	24	18
Percentage of troposphere occupied by layers	17.0	16.6	16.3	19.8	19.5	15.4	24.3	19.0	17.6
Number of layers per profile	1.79	1.76	1.48	1.54	1.65	1.43	2.08	1.25	1.70
Thickness, m (Mean, median)									
Type 1	639 (406)	663 (394)	721 (483)	743 (507)	751 (433)	640 (398)	692 (342)	821 (538)	691 (426)
Type 2	806 (542)	758 (506)	857 (510)	942 (632)	1064 (704)	1025 (688)	1015 (665)	954 (670)	854 (566)
Type 3	746 (545)	835 (580)	818 (555)	843 (649)	854 (698)	591 (413)	762 (577)	738 (494)	780 (564)
Type 4	636 (451)	680 (498)	689 (505)	837 (570)	785 (549)	792 (602)	634 (472)	847 (606)	714 (508)
Altitude, km (Mean, median)									
Type 1	6.7 (6.9)	6.2 (6.3)	5.9 (6.1)	5.6 (5.4)	6.2 (5.9)	5.6 (5.4)	6.3 (6.3)	5.5 (5.3)	6.2 (6.3)
Type 2	5.7 (5.6)	5.5 (5.2)	5.8 (5.6)	5.3 (5.2)	6.1 (6.1)	6.1 (6.2)	6.1 (6.1)	5.7 (5.6)	5.7 (5.6)
Type 3	5.9 (6.0)	6.0 (6.2)	6.1 (6.3)	5.7 (5.6)	5.1 (4.7)	5.1 (4.0)	5.9 (5.1)	5.8 (5.4)	5.9 (5.8)
Type 4	6.0 (6.2)	5.8 (5.8)	6.0 (5.8)	5.8 (5.7)	6.0 (6.0)	6.4 (6.9)	6.6 (6.9)	5.9 (5.9)	6.0 (6.0)
Number of profiles	5869	2164	1129	721	1025	606	262	1421	13809

MOZAIC data from September 1994 to December 1997. Minimum O₃ deviation is 10 ppbv, and minimum H₂O deviation is 5%. Both the mean and median values (the latter in parentheses) are given for the thickness and altitude of layers.

profiled when the tropopause was reached (according to the temperature definition). A full description of the procedure used for defining the constituent background is given by *Stoller et al.* [1999].

As previously done, we assume the aircraft measurements during ascent and descent to be vertical profiles. There is, of course, the possibility that horizontal structures could be aliased into "vertical" structures. With a one-dimensional measurement it is impossible to completely unravel this ambiguity. In general, we rely on the very large horizontal-to-vertical aspect ratio of the atmosphere. However, comparisons with ozonesondes (which ascend more steeply than aircraft) [*Thouret et al.*, 1998a] and lidar (which provide a two-dimensional coverage of layers) [*Stoller et al.*, 1999] have shown that the assumption of vertical profiling by aircraft is quite good. Of course, there will be some amount of noise introduced into the layer statistics due to this assumption, but we have no reason to believe that the noise will be biased for key statistics, such as the percentages of the types of layers.

3. General Characteristics and Regional Differences

Because the MOZAIC program provides data almost worldwide, we are now able to identify the regional differences in the occurrence of the layers. Table 1 gives some general characteristics of the tropospheric layers: (1) number of observations in each category, (2) percentage of observations in each category, (3) percentage of the troposphere occupied by layers, (4) average number of layers per profile, (5) mean thickness and mean height for each type of layer, and (6) indication of the number of MOZAIC profiles for each region described here. These refer to the whole set sampled by MOZAIC aircraft during the first 3.5 years of the program.

As noticed previously by *Newell et al.* [1999], who compared statistical results between MOZAIC (collected almost everywhere but the Pacific region) and three PEM data sets (collected only in the Pacific region), there are no real regional differences in the general characteristics of these layers. When considering only MOZAIC data, we still notice that type 2 is the most abundant everywhere (45–54%, with a maximum in Europe). Seventeen percent of the troposphere is occupied by layers (15–24%), equivalent to an average of 1.70 (1.43–2.08) layers per profile. Notice, though, that tropical Africa is only represented by 262 vertical profiles for the period April–December, 1997. The mean altitude of the layers is between 5 and 6 km, and the mean thickness is about 600–1000 m. However, we notice a big difference between the mean and the median values of the thickness. Histograms including the natural logarithm of the thickness will be shown and discussed in the next section, and they illustrate that half of the layers are less than 500 m thick. If we consider the mean value, we notice that the type 2 layers are the thick-

est layers everywhere but in the eastern United States and are globally thicker in the tropical and subtropical latitudes than at midlatitudes. The differences in median are not so obvious, especially for types 2 and 3 at midlatitudes. That type 2 layers are thicker than the others is an argument in favor of the trapping process, as already suggested by *Stoller et al.* [1999]. Sometimes layers defined as type 2 are a combination of pollution from the boundary layer and stable stratospheric air on top of it, thus giving a thicker layer than a pure polluted layer or a pure stratospheric intrusion.

As a remark, we have to be aware that MOZAIC aircraft sample the atmosphere from 0 to 12 km altitude and our study deals with layers observed between 2 km altitude and either 12 km altitude or the tropopause. So at midlatitudes, all the troposphere is sampled, but in the tropics only 75% (12 km/16 km) of the troposphere is sampled. Thus we could argue that there are more layers in the tropics that are unobserved than at midlatitudes. In any case, layers are a common tropospheric feature, as already presented by *Newell et al.* [1999], and we are now able to present the general characteristics of these layers with the most appropriate data set currently available.

Figures 1, 2, and 3 present the general characteristics of the layers. The histograms have been plotted using the whole MOZAIC data set. Figure 1 gives the altitude distribution for the four types of layers. Even if the mean altitude is about the same for every type of layer (between 5 and 6 km altitude, as shown in Table 1), types 1 and 3 present many more layers close to the 2 km lower-altitude limit than the two other types. That is probably due only to the fact that types 1 and 3 (moist layers) have a surface source while types 2 and 4 (dry layers) have an upper tropospheric source. Even if Types 2 and 4 have a boundary layer origin, they must have passed through the upper troposphere to make them drier. In the potential temperature (θ) distribution (Figure 2), we observe more Gaussian distributions centered at about 315–320 K for all categories, which is a little bit higher than (but still in agreement with) what *Iselin and Gutowski* [1997] found studying only water vapor layers. This was not the case for the altitude distributions, so it may imply an isentropic transport for the layers. The thickness distributions (Figure 3) look alike for each type of layer, and as mentioned previously, we note that most of the layers are thinner than average. The median values are about 500 m for each type of layer (see Table 1 for precise values). Figure 4 gives the histograms of the natural logarithm of the thickness. The distributions now appear Gaussian, and the means and medians at about 6.0–6.3 (about 400–550 m) for the four types of layers are better defined.

We can also assess the meridional variations using this data set. Figure 5 gives the altitude and thickness means (in both altitude and potential temperature coordinates) versus latitude. Statistical results have been

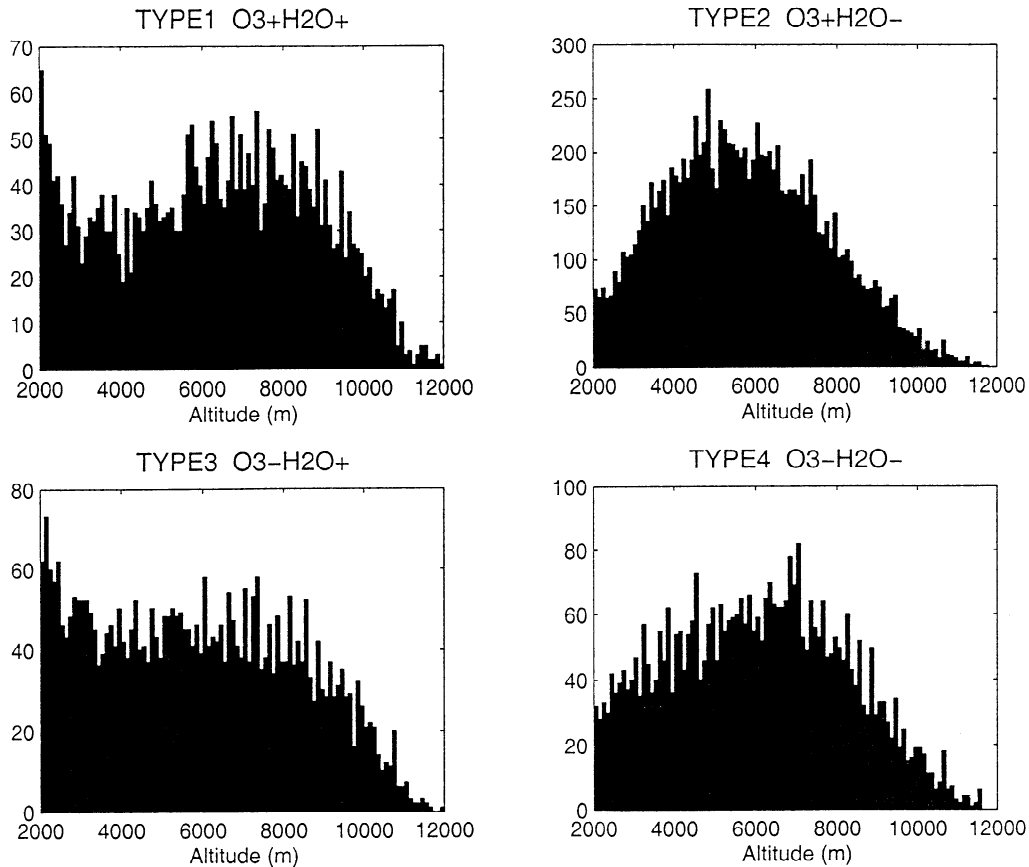


Figure 1. Histogram of the altitude distribution for the four types of layers, from the whole Measurement of Ozone and Water Vapor by Airbus In-Service Aircraft (MOZAIC) data set.

computed for five different latitude bands: 25°S – 5°N , 5°N – 15°N , 15°N – 25°N , 25°N – 35°N , and 35°N – 50°N , covering thus all the airports documented by MOZAIC aircraft. The distributions in Figures 1–4 are quite similar (shape-wise) from one region to another, but Figure 5 reveals differences in midlatitudes versus tropics. As noticed in Table 1, type 2 layers are the thickest layers everywhere (probably characteristic of the trapping process). In terms of potential temperature, each type of layer is globally thicker at lower latitudes, as emphasized by the plot giving the thickness in kelvins. The troposphere is globally less stable in the tropics, and so layers can spread out more vertically in the tropics than at midlatitudes. The latitudinal variation of the mean altitude does not show a clear trend. Plotted against θ , the layers appear to be “higher” (i.e., greater absolute value for θ) in the troposphere at low latitudes than at midlatitudes. At first this may seem to contradict the isentropic latitudinal long-range transport hypothesis, because we would have expected no variation in mean θ versus latitude. However, since we avoid the first 2 km of the troposphere and the lower stratosphere, we cannot define layers with potential temperature lower than ~ 310 K in the tropics or greater than ~ 330 K at midlatitudes, resulting thus in a lower mean value at midlatitudes.

4. Seasonal Variations

The PEM data gave a lot of information about the layers and their probable origins. With 3.5 years of regular measurements the MOZAIC program allows us now to investigate the seasonal variations of these layers. We will show statistical results for the whole MOZAIC data set and for three particular regions. In order to avoid any problems related to the representativity of the data, we will only focus on the analysis of the seasonal variations of the two most documented regions at midlatitudes (Europe and the eastern United States) and the most documented tropical region (Southeast Asia). There were about 6000, 2000, and 1000 ozone and water vapor vertical profiles for Europe, eastern United States, and tropical Asia, respectively (see Table 1).

An important criterion to analyze is what we call “percentage of the troposphere occupied by layers” corresponding to the sum of the thicknesses divided by the total kilometers profiled. As seen previously, this number is about 17% of the 2–12 km range in the troposphere. Figure 6 presents the seasonal variations of this number for the whole MOZAIC data set and for the three selected regions. Then, we can see that this part of the troposphere occupied by layers goes from 7 to 33% depending on the region and on the season,

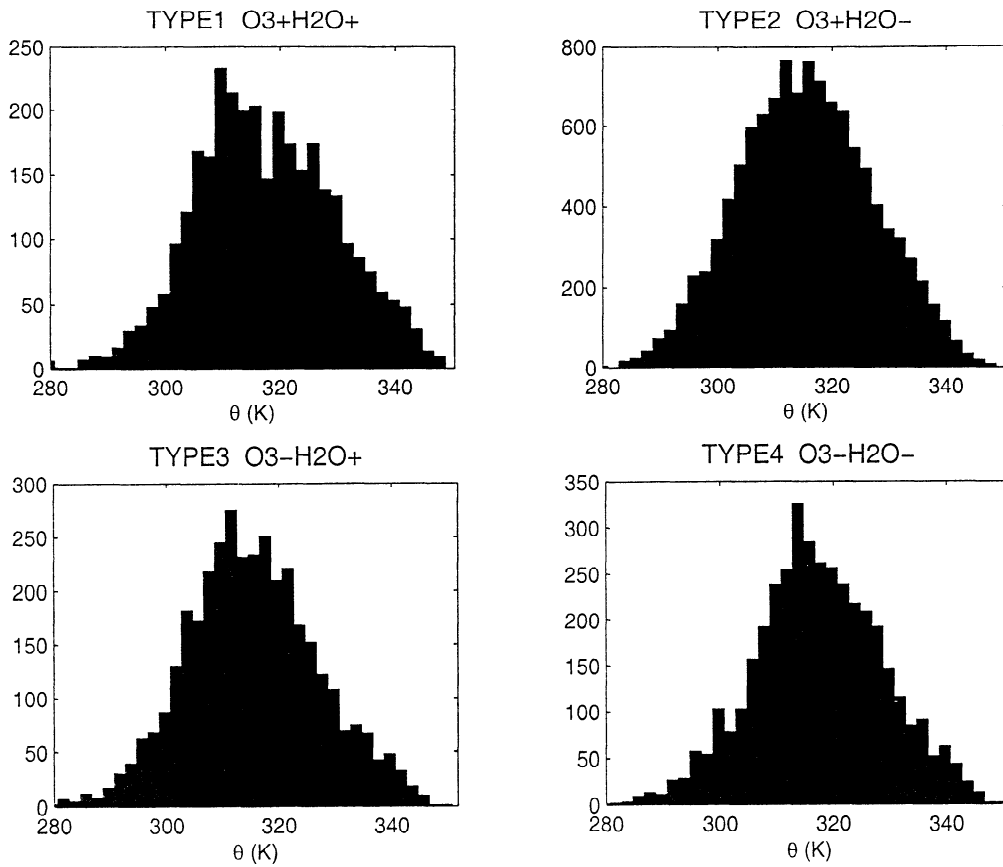


Figure 2. Histogram of the potential temperature distribution for the four types of layers, from the whole MOZAIC data set.

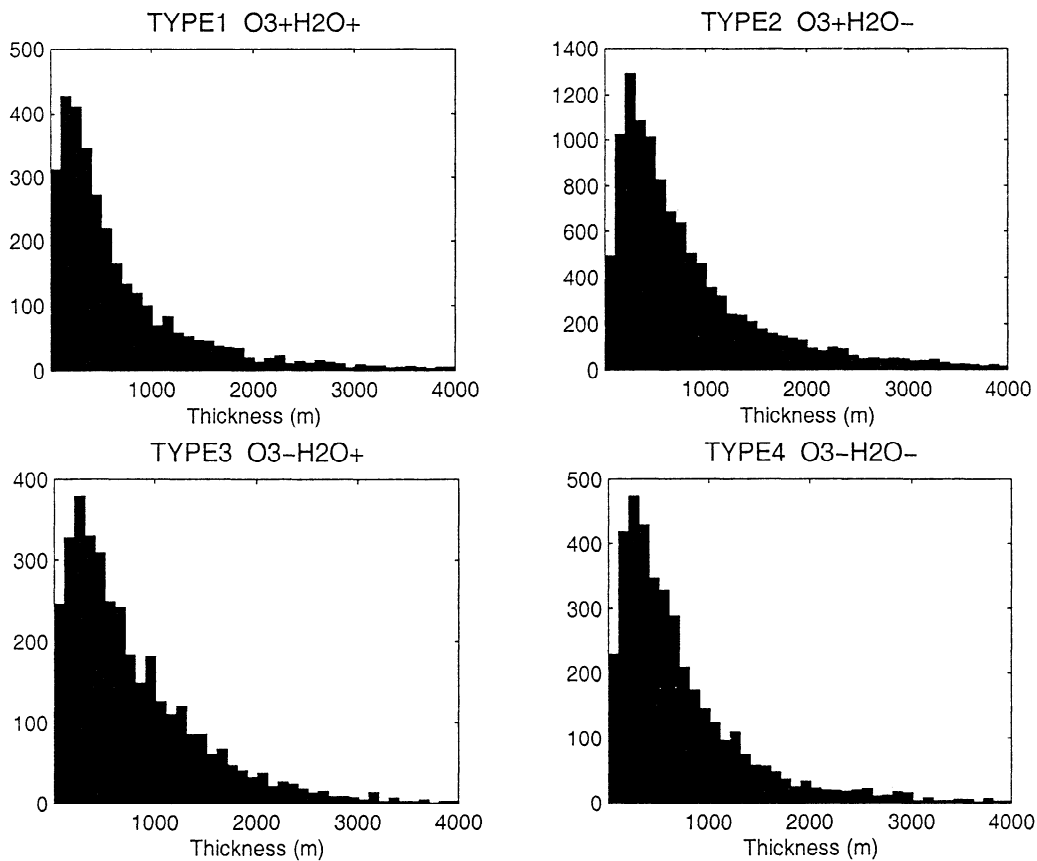


Figure 3. Histogram of the thickness distribution for the four types of layers, from the whole MOZAIC data set.

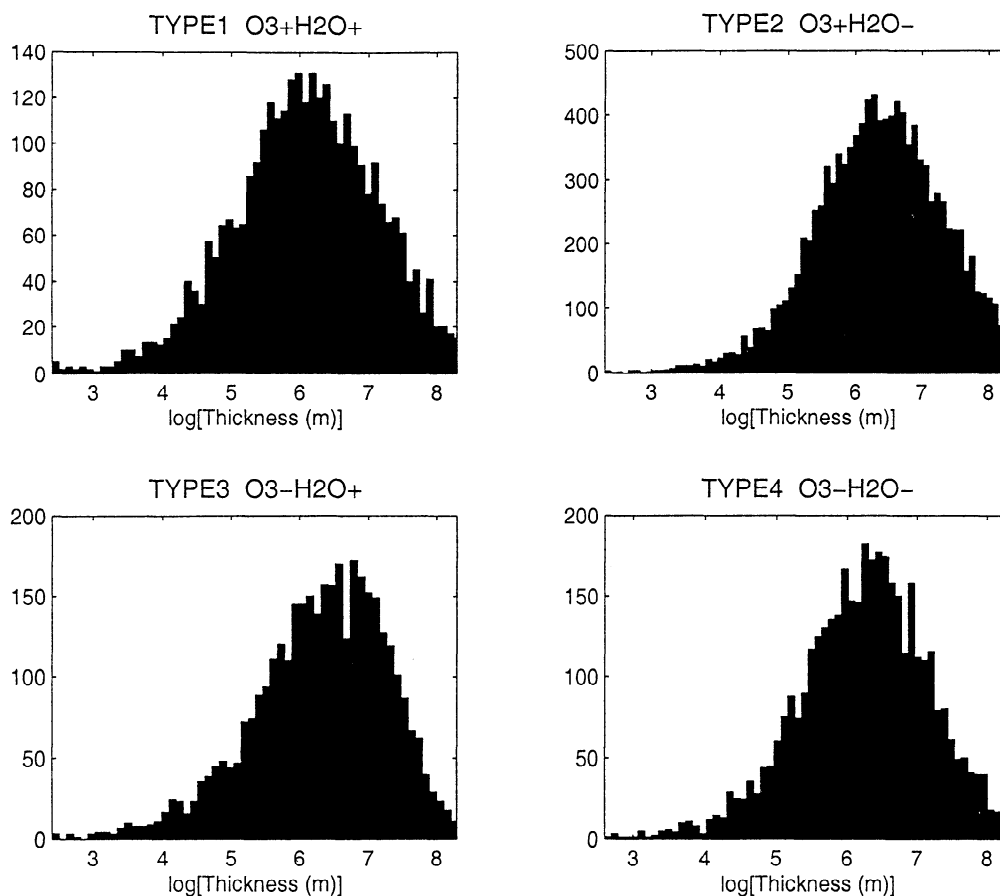


Figure 4. Histogram of the natural log thickness distribution for the four types of layers, from the whole MOZAIC data set.

with a maximum in summer for the midlatitudes and a maximum in spring for tropical Asia. Figure 6 also gives the number of layers per profile (multiplied by 10 for easier viewing on this plot). First, we notice that these two quantities present exactly the same seasonal cycle everywhere. So we deduce that there is no seasonal cycle for the thickness of the layers. Layers are as thick or thin in winter as in summer. Finally, Figure 6 also gives an indication of the relative number of profiles without any layer. It is interesting to notice the completely opposite seasonal cycle. This means that more no-layer profiles may occur in winter at midlatitudes because sources of excess ozone and moisture are weaker, the mechanism generating layers is weaker, or processes maintaining layers after generation are less effective. Stronger vertical mixing would be one factor making layer maintenance less effective.

Figure 7 is an extension of Figure 6 in the sense that it also represents the number of layers per profile and the decomposition in each type of layer for the entire MOZAIC data set and for the three selected regions. We know that globally we observe more layers in summer than in winter at midlatitudes. Is there any seasonal behavior for each different type of layer? The answer is no, because each layer category follows exactly

the same cycle as the total number of layers. This means that there is no seasonal cycle in the fraction of layers falling into each category. Type 2 (stratospheric intrusions and/or continental pollution) is the most abundant everywhere for every season. Considering averages for the whole MOZAIC data set, the percentage of observations in type 2 is always greater than 47% and can reach 56%. Only 13–23% of observations are classified in any of the three other types. For both Europe and the eastern United States we observe a strong summer maximum in the total number of layers, with a factor of 4 between the minimum in January and the maximum in July. Summer at northern midlatitudes is the period of the most intensive ozone photochemical production, and because of that, the seasonal cycle of the mean ozone concentration in the free troposphere also presents a summer maximum [Thouret *et al.*, 1998b], and given that type 2 is the most abundant, we can hypothesize that stratospheric air mixed with pollution is the dominant subtype of layer. It also means that stratospheric intrusions are not negligible in summer at northern midlatitudes. Summer at midlatitudes is also the season of more intensive convection, giving then an additional source for creating layers. For example, convection can raise pollution from the ground,

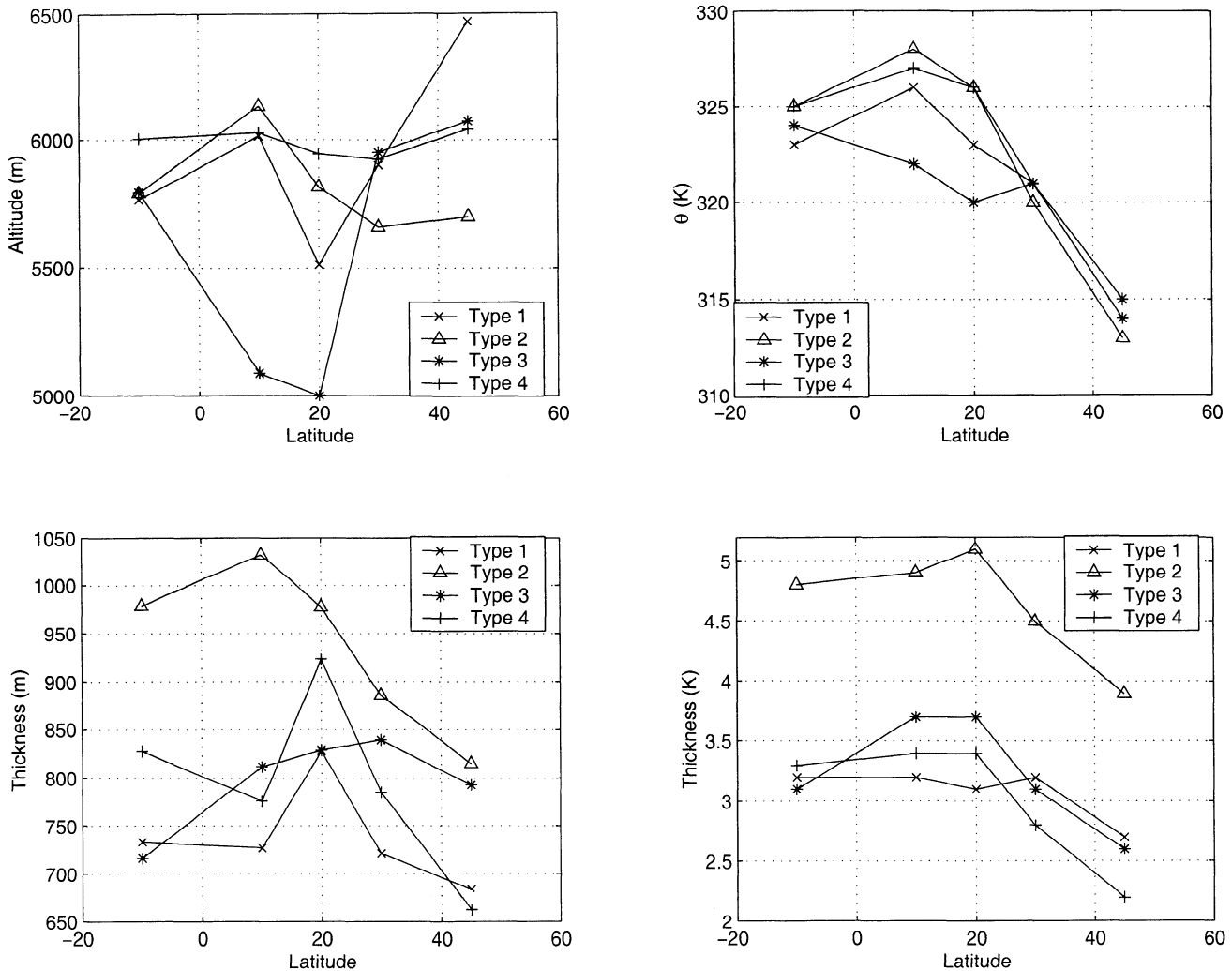


Figure 5. Latitudinal variations of altitude and median thickness expressed in both meters and potential temperature in Kelvin coordinates for five latitude bands, from the whole MOZAIC data set.

and then stable air masses likely coming from the lower stratosphere can trap the polluted plume and force it to spread out horizontally.

In tropical Asia we observe a spring maximum and a secondary peak in June, and as for midlatitudes, we notice the same behavior for each category of layers. Once again, spring is the period of intensive biomass burning in this region [Hao and Liu, 1994], and the seasonal cycle of the ozone concentrations in the free troposphere also presents a spring maximum [Chan *et al.*, 1998; V. Thouret *et al.*, manuscript in preparation, 2000]. Type 2 is also the most abundant, and we can argue that the main mechanism for creating layers is buoyant pollution capped by stratospheric air. When looking at all individual MOZAIC profiles in the region, we notice that in February, for example, most of the profiles contain two layers in the troposphere (see Figure 8, top). The first one is observed at about 2–3 km altitude, with high ozone and high water vapor thought to be due to biomass burning in the local area (as al-

ready observed by Liu *et al.* [1999] over Hong Kong, for example), and another one is observed at about 5–6 km altitude, with high ozone and low water vapor probably due, when looking at back trajectories (not shown here though), to long-range transport of polluted air masses either from biomass burning in Africa or from the stratosphere. The secondary peak in June cannot be explained this way. June is the beginning of the summer monsoon. Thus we often observe flat profiles with low ozone values throughout the troposphere, revealing the intense vertical mixing. On the other hand, we also observe a number of profiles with very low ozone values throughout the troposphere up to 6–8 km altitude, and above we find high to very high ozone values probably corresponding to stratospheric intrusions or continental pollution (Figure 8, bottom). This $O_3 + H_2O$ -layer might have been produced farther north and then transported through the anticyclone present in this season in the region. Figures 6 and 7 showed that there is no seasonal cycle for thickness and for the ratio of

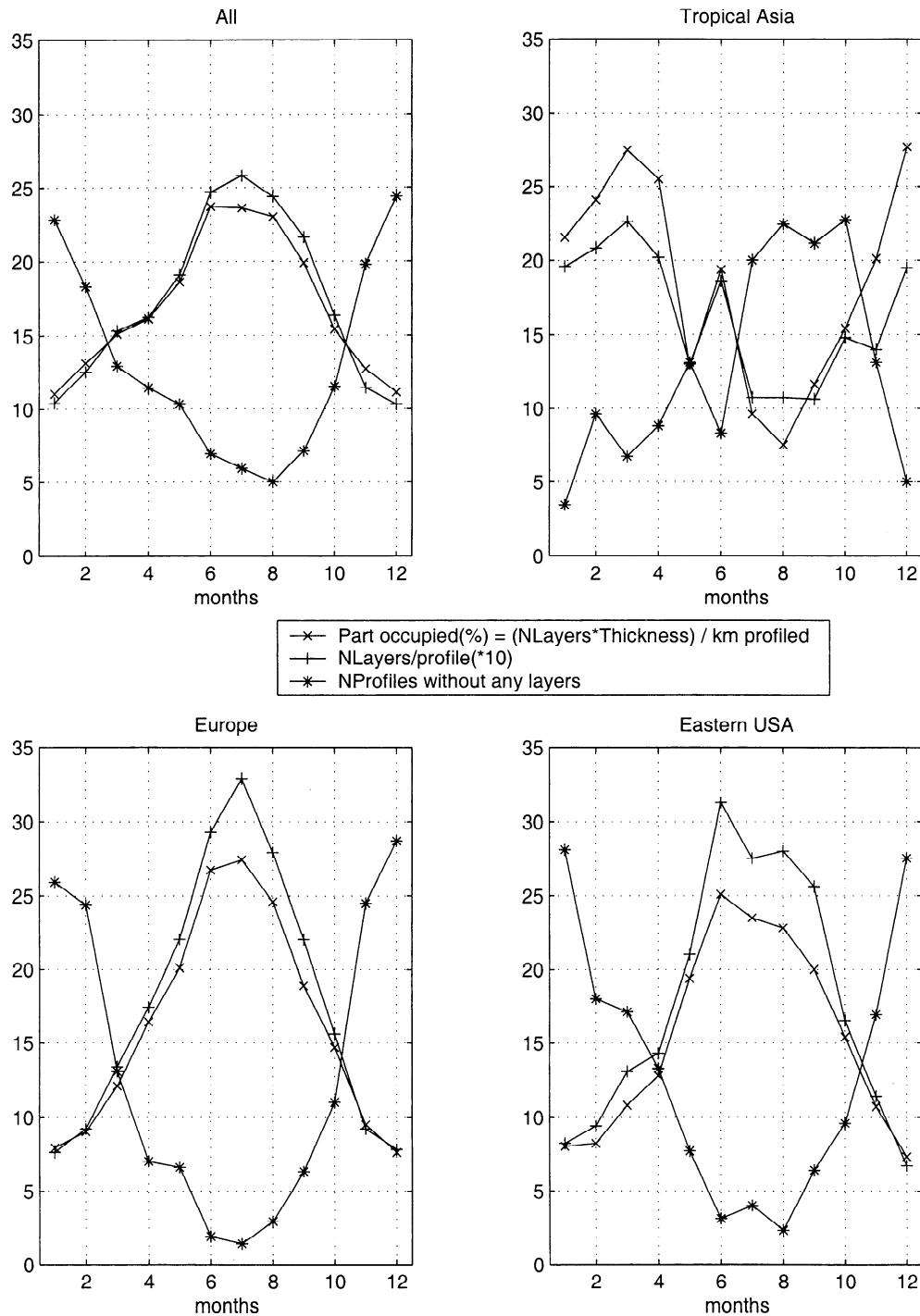


Figure 6. Percentage of the troposphere occupied by layers, number of layers per profile (multiplied by 10 for easier viewing), and relative number of profiles without any layers, calculated for the whole MOZAIC data set and for the three selected regions.

observations in each category. Only the number of layers per profile present a strong seasonal cycle, with a maximum in summer at midlatitudes and in spring in tropical Asia. To look for any altitude dependence for the occurrence of layers, Figure 9 gives the number of layers per kilometer profiled for five ranges between 2 and 12 km altitude for the whole MOZAIC data set and the three selected regions. We used the quantity “num-

ber of layers per kilometer profiled” to give a reliable number of layers independent of the number of profiles. This is particularly important for the last altitude range (10–12 km) because some profiles (almost half of them) do not reach the 12 km top altitude. As we noticed with thickness, Figure 9 reveals the lack of any seasonal cycle for the altitude of the layers. At any altitude level the number of layers presents a maximum in summer

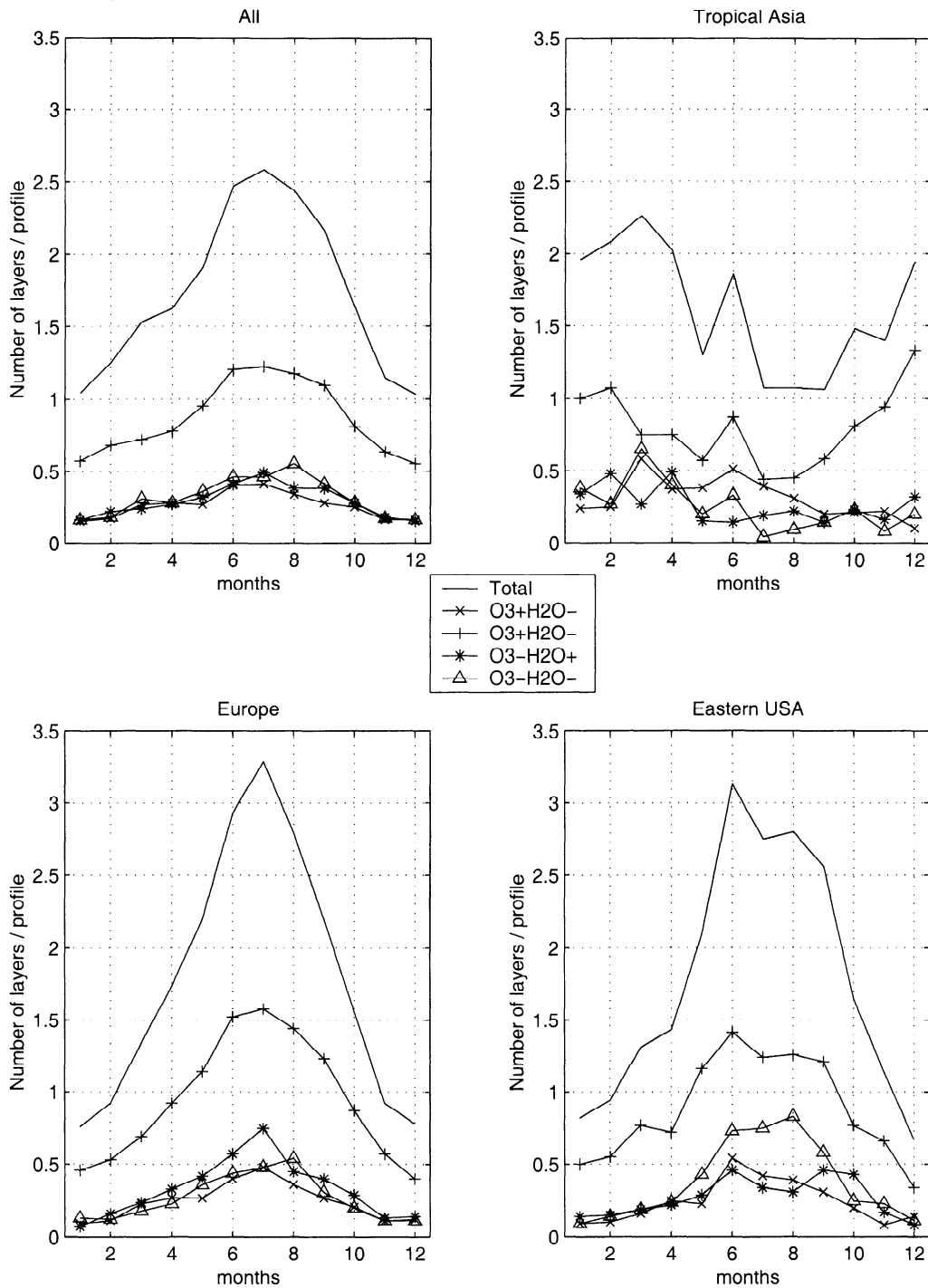


Figure 7. Total number of layers per profile and decomposition in each category, calculated for the whole MOZAIC data set and for the three selected regions.

at midlatitudes and in spring in tropical Asia. As noticed previously with the distributions (Figure 1), the largest numbers of layers are found between 4 and 8 km altitude, somewhat fewer are found at either 2–4 km or 8–10 km, and only a few layers are found at 10–12 km.

Finally, we have to keep in mind that the layers are detected through ozone deviations. In that sense, it is not very surprising to notice that the number of layers per profile follows the same seasonal cycle (the same

shape) as the ozone concentrations in the free troposphere for every region considered in this study. To identify layers through our algorithm, we need a rather big enhancement in the ozone concentrations compared with the background (for O_3+ layers) or a rather high background compared with the real profile to be able to notice O_3- layers. This is probably why we observe a maximum of layers in summer at midlatitudes or in spring in tropical Asia. It also probably means that

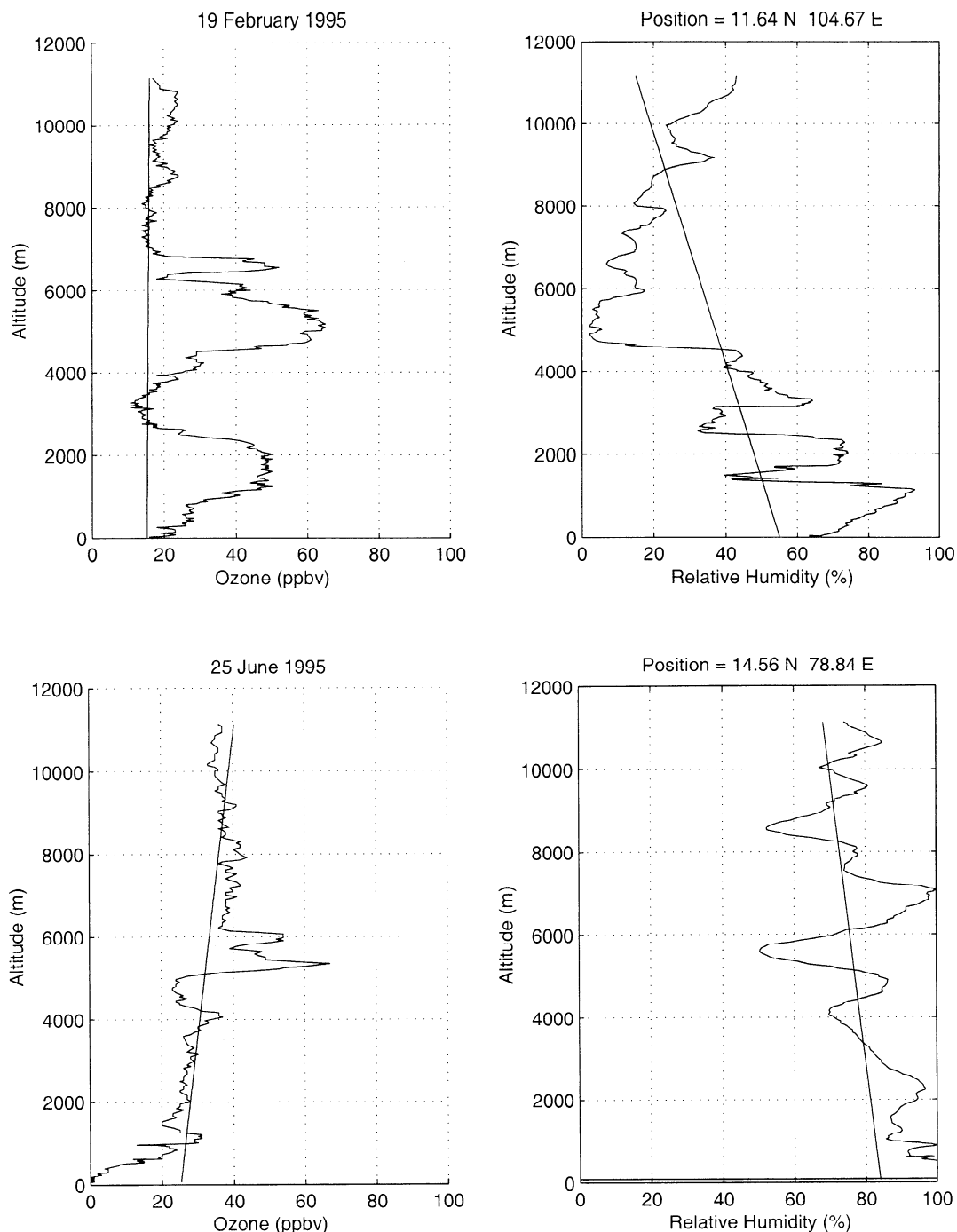


Figure 8. Examples of ozone and water vapor vertical profiles and corresponding calculated background in tropical Asia in (top) February and (bottom) June.

we miss many layers only because they have no ozone signatures. The tropospheric layers as defined in this study require a dynamical source to create the layer itself and an ozone signature to be depicted by our algorithm. The use of another tracer, with a different seasonal cycle, could lead to another seasonal cycle for the number of layers per profile. From January 2000 on, MOZAIC III will provide CO measurements. We look forward to seeing the new results including 1 year of O_3 , H_2O , and CO measurements. Moreover, additional

CO measurements will give us the opportunity to distinguish stratospheric intrusions from pollution or from pollution trapped by stratospheric air within the type 2 layers.

5. Stability Criteria

To go further in identifying the physical mechanisms responsible for the formation and development of the layers, we analyzed potential temperature profiles in

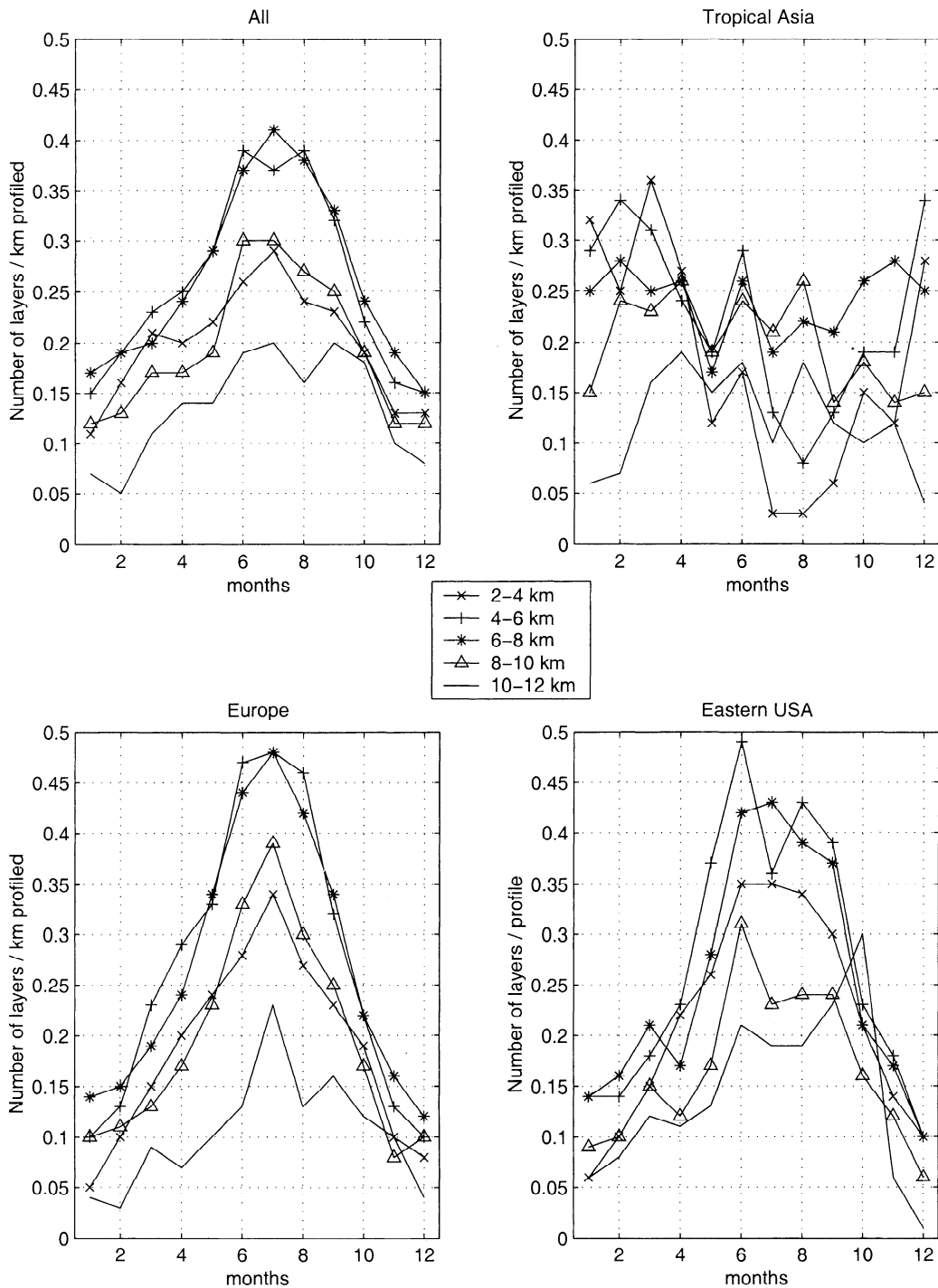


Figure 9. Total number of layers per kilometer profiled for each altitude range, calculated for the whole MOZAIC data set and for the three selected regions.

order to compare the gradient inside and outside the layers. As for ozone and water vapor, we defined automatically a background profile for each potential temperature profile. This background corresponds to the fitted lines for three altitude ranges (2–5, 5–8, and 8–12 km). We used three background profiles because the general trends in potential temperature profiles change with height. Then we compared the gradients for the

bottom half (dry layers) or top half (wet layers) of the layer and outside the layer. As calculated by *Stoller et al.* [1999] and *Newell et al.* [1999], dry layers give a relative radiative cooling near the layer base and a radiative heating near the top, thus stabilizing the air in the layer and preventing vertical mixing across the layer, while it is the contrary for wet layers. In this way we obtain a new set of layer types, with each one of the

Table 2. Percentage of Layer Types Categorized Versus Stability

Layer Type	Higher Stability	Lower Stability
Type 1 (O ₃ + H ₂ O+)	8%	7%
Type 2 (O ₃ + H ₂ O-)	34%	17%
Type 3 (O ₃ - H ₂ O+)	7%	9%
Type 4 (O ₃ - H ₂ O-)	8%	10%

previous ones divided into high or low stability within the layer, meaning that the static stability within the layer was higher or lower than the one corresponding to the background. The results calculated for the whole MOZAIC data set are given in Table 2.

We see that this new criterion of stability is not very meaningful for types 1, 3, and 4 because we obtain a similar decomposition in each category. For type 2, though, it appears clearly that most of the observed layers (34% versus 17%) have a higher stability than the environment outside the layer. This is not really surprising if we interpret stability as a “subsidence tracer.” Type 4, however, does not reveal such a feature (8% versus 10%). This new finding could be a strong argument for stratospheric intrusions helping create type 2 layers. Stability is obviously not the ideal tracer for stratospheric intrusions but gives nevertheless a very good idea, as demonstrated by *Cho et al.* [1999b] studying two cases of tropopause folding during the NASA Subsonics Assessment (SASS) Ozone and Nitrogen Experiment (SONEX) mission. *Cho et al.* [1999b] found a very good correlation in time and space between ozone and stability throughout the tropopause folding event. To go further in the analysis, we plan to use PV profiles as a stratospheric tracer, and apply our automatic algorithm for each individual PV vertical profile and obtain in this way a new set of layers. If we obtain, for example, the type O₃+ H₂O- PV+ as the most abundant type of observed layer, it would be another strong argument for stratospheric intrusions as the main mechanism responsible for creating layers.

6. Discussion

For the first time, we now have more extensive knowledge of these tropospheric layers in terms of their general characteristics at a global scale. Everywhere, all the time, stable O₃+ H₂O- layers are the most common type. These layers, as well as the others are mostly present between 4 and 8 km altitude, with a thickness of about 500 m. The most surprising feature in this study is the lack of any seasonal variations. The only seasonal cycle and regional difference observed concern the average of the number of layers per profile (strong maximum in summer at midlatitudes and in spring in tropical Asia). The relevant physical mechanisms are not clear then. For type 2, for example, it is still very difficult to

discriminate between pure stratospheric intrusions and pure subsiding pollution. We think it might be a combination of the two processes that we could call “pollution with a stratospheric cap,” meaning that pollution can be raised by convection and then spread out horizontally, trapped by stable air originating from the stratosphere. As defined previously dealing with the three previous PEM data, type 2A (O₃+H₂O-CO-CH₄+) is the most abundant everywhere in these missions (24–32% of the observations) and corresponds to aged pollution, but “stratospheric air, sometimes mixed with trapped pollution, was the dominant layers source in all three missions” [*Stoller et al.*, 1999, p. 5745]. Therefore types 1 and 2 are not easily separated. This new finding reveals then that stratospheric intrusions (or at least their influence) are not negligible in summer at midlatitudes or in the tropics, as previously thought. Such conclusions have been already drawn by *Chen* [1995]. Using a semi-Lagrangian transport model and analyzed winds from the European Centre for Medium-Range Weather Forecasts, it is found that on the 330-K isentropic surface and below (the domain sampled in this study), stratosphere-troposphere exchange occurs vigorously in all seasons, caused mainly by the irreversible mixing and transport by breaking synoptic-scale baroclinic disturbances. More accurately, according to *Postel and Hitchman* [1999], tropopause folding due to Rossby waves breaking at 350 K present an occurrence maximum in summer at northern midlatitudes with a factor of 5 between July and January. This is in complete agreement with the number of layers per profile (same summer maximum with a factor of 4 between July and January at northern midlatitudes), giving then another argument in favor of stratospheric intrusions for helping the creation of layers.

Types 3 and 4, which may be associated with convection over the ocean, are also difficult to separate. In respect to mass conservation, convection and subsidence may be seen as coupled ascending and descending motions even if the two parts do not occur in the same area.

From the MOZAIC data set we now have a first assessment of the behavior of layers in the troposphere. To go further and really assess the physical mechanisms involved, we still need new inputs in this huge database. We plan to use PV profiles calculated for each MOZAIC profile by Centre National de Recherches Météorologiques. The next phase of the MOZAIC program will start in January 2000 and provide regular measurements of CO, as well as of ozone and water vapor. Thus we will be able to discriminate more accurately between the stratosphere and pollution. If we are to recommend that three-dimensional chemical and transport models (3-D CTMs) should reproduce this phenomenon, we still have to try to answer more accurately these types of questions: Why do we find most of the layers between 4 and 8 km altitude? Why are half of the observed layers O₃+H₂O-? What are the physi-

cal mechanisms involved in the creation of these layers? We have given here the beginning of an answer. Tropospheric ozone layers are mostly found in the middle troposphere, where convection from the boundary layer and intrusions from the stratosphere or large-scale subsidence meet. The predominance of O_3+H_2O - layers reveals both of the two major sources of tropospheric ozone and probably affects the overall mass balance between the troposphere and the lower stratosphere. The main physical mechanisms involved for creating layers are thought to be stratospheric intrusions and convection and also probably both of them coupled. To learn more about them and about the lifetime of the layers, however, and their extent and motion, we have started case studies. This paper deals only with the statistical results of layer distributions and behavior from the most extensive data set currently available.

This real property of the troposphere needs to be explored in detail, and a good assessment of the layers could lead us to a better empirical assessment of the different tropospheric ozone sources. One of the main uncertainties in the current 3-D CTMs is the ozone flux into the troposphere from the stratosphere. Being able to assess this flux through the mass of ozone involved in the layers could give us a better estimate of the natural tropospheric ozone source, which has important implications for atmospheric chemistry. Another main interest of this study is related to the large-scale dynamics of the atmosphere, and further development could provide an assessment of the PV fluxes in the troposphere.

Acknowledgments. The MIT work was funded by NSF grant ATM-9910244 and NASA grant NAG1-2173. We thank Air France, Lufthansa, Austrian Airlines, and Sabena for carrying the MOZAIC equipment free of charge and for performing the maintenance.

References

- Bernard, R., Sodium in the high atmosphere, *Nature*, *141*, 788, 1938.
- Chan, L. Y., H. Y. Liu, K. S. Lam, T. Wang, S. J. Oltmans, and J. M. Harris, Analysis of the seasonal behavior of tropospheric ozone at Hong Kong, *Atmos. Environ.*, *32*, 159–168, 1998.
- Chen, P., Isentropic cross-tropopause mass exchange in the extratropics, *J. Geophys. Res.*, *100*, 16,661–16,673, 1995.
- Cho, J. Y. N., R. E. Newell, V. Thouret, A. Marengo, and H. G. Smit, Trace gas study accumulates 40 million frequent-flyer miles for science, *Eos Trans. AGU*, *80*, 377–384, 1999a.
- Cho, J. Y. N., et al., Observations of convective and dynamical instabilities in tropopause folds and their contribution to stratosphere-troposphere exchange, *J. Geophys. Res.*, *104*, 21,549–21,568, 1999b.
- Danielsen, E. F., R. S. Hipskind, W. L. Starr, J. F. Veder, S. E. Gaines, D. Kley, and K. K. Kelly, Irreversible transport in the stratosphere by internal waves of short vertical wavelength, *J. Geophys. Res.*, *96*, 17,433–17,452, 1991.
- Hao, W. M., and M.-H. Liu, Spatial and temporal distribution of tropical biomass burning, *Global Biogeochem. Cycles*, *8*, 495–503, 1994.
- Helten, M., H. G. J. Smit, W. Sträter, D. Kley, P. Nédélec, M. Zöger, and R. Busen, Calibration and performance of automatic compact instrumentation for the measurement of relative humidity from passenger aircraft, *J. Geophys. Res.*, *103*, 25,643–25,652, 1998.
- Iselin, J. P., and W. J. Gutowski, Water vapor layers in STORM-FEST rawinsonde observations, *Mon. Weather Rev.*, *125*, 1954–1963, 1997.
- Liu, H., W. L. Chang, S. J. Oltmans, L. Y. Chan, and J. M. Harris, On springtime high ozone events in the lower troposphere from southeast Asian biomass burning, *Atmos. Environ.*, *33*, 2403–2410, 1999.
- Marengo, A., et al., Measurement of ozone and water vapor by Airbus in-service aircraft: The MOZAIC airborne program, An overview, *J. Geophys. Res.*, *103*, 25,631–25,642, 1998.
- Muschinski, A., and C. Wode, First in-situ evidence for co-existing sub-meter temperature and humidity sheets in the lower free troposphere, *J. Atmos. Sci.*, *55*, 2893–2906, 1998.
- Newell, R. E., Z.-X. Wu, Y. Zhu, W. Hu, E. V. Browell, G. L. Gregory, G. W. Sachse, J. E. Collins Jr., K. K. Kelly, and S. C. Liu, Vertical fine-scale atmospheric structure measured from NASA DC-8 during PEM-West A, *J. Geophys. Res.*, *101*, 1943–1960, 1996.
- Newell, R. E., V. Thouret, J. Y. N. Cho, P. Stoller, A. Marengo, and H. G. Smit, Ubiquity of quasi-horizontal layers in the troposphere, *Nature*, *398*, 316–319, 1999.
- Newman, P. A., and M. R. Schoeberl, A reinterpretation of the data from the NASA stratosphere-troposphere exchange project, *Geophys. Res. Lett.*, *22*, 2501–2504, 1995.
- Postel, G. A., and M. Hitchman, A climatology of Rossby wave breaking along the subtropical tropopause, *J. Atmos. Sci.*, *56*, 359–372, 1999.
- Stoller, P., et al., Measurements of atmospheric layers from the NASA DC-8 and P-3B aircraft during PEM-Tropics A, *J. Geophys. Res.*, *104*, 5745–5764, 1999.
- Thouret, V., A. Marengo, J. Logan, P. Nédélec, and C. Grouhel, Comparisons of ozone measurements from the MOZAIC airborne program and the ozone sounding network at eight locations, *J. Geophys. Res.*, *103*, 25,695–25,720, 1998a.
- Thouret, V., A. Marengo, P. Nédélec, and C. Grouhel, Ozone climatologies at 9–12 km altitude as seen by the MOZAIC airborne program between September 1994 and August 1996, *J. Geophys. Res.*, *103*, 25,653–25,679, 1998b.
- Wu, Z.-X., R. E. Newell, Y. Zhu, B. E. Anderson, E. V. Browell, G. L. Gregory, G. W. Sachse, and J. E. Collins Jr., Atmospheric layers measured from the NASA DC-8 during PEM-West B and comparison with PEM-West A, *J. Geophys. Res.*, *102*, 28,353–28,365, 1997.
- J. Y. N. Cho, R. E. Newell, and V. Thouret, Department of Earth, Atmospheric, and Planetary Sciences, Massachusetts Institute of Technology, 77 Massachusetts Avenue, Room 54-1823, Cambridge, MA 02139-4307. (jcho@pemtropics.mit.edu; renewell@mit.edu; valerie@pemtropics.mit.edu)
- A. Marengo, Laboratoire d'Aérodologie, Observatoire Midi-Pyrénées, UMR 5560, Université Paul Sabatier, 14 Avenue Edouard Belin, 31400 Toulouse, France. (mara@aero.obs-mip.fr)
- H. G. J. Smit, Forschungszentrum Jülich, Institut für Chemie der Belasten Atmosphäre, Department für Chemie und Dynamik der Geosphäre, 52425 Jülich, Germany. (h.smit@kfa-juelich.de)

(Received December 20, 1999; revised April 7, 2000; accepted April 12, 2000.)